Supplementary information

Table S1. Cross-spectral analyses of *G. ruber* Mg/Ca-SST obtained for core MD05-2920 relative to benthic foraminiferal $\delta^{18}O$ records over different orbital bands

Orbital band	Coherency (lower/higher)	Phase (º)	Phase (kyr)
C. wuellerstorfi $\delta^{18}O$			
100 kyr	0.99 (0.94/1.00)	12.7±10.3	3.5±2.8
41 kyr	0.95 (0.80/0.99)	2.3±5.1	0.3±0.6
23 kyr	0.98 (0.91/0.99)	2.2±0.9	0.1±0.1
U. peregrina $\delta^{18}O$			
100 kyr	0.99 (0.94/1.00)	12.6±10.1	3.5±2.8
41 kyr	0.95 (0.82/0.99)	3.4±4.7	0.4±0.5
23 kyr	0.97 (0.90/0.99)	2.1±1.3	0.1±0.1

Analyses were carried out using the Blackman-Tukey method with a bandwidth of 0.010 kyr^{-1} and a confidence interval of 95%. No-zero coherence > 0.603.

Table S2. Cross-spectral analyses of bottom water temperature changes (ΔBWT) obtained for core MD05-2920 and for ODP1123 (Elderfield et al., 2012) relative to sea salt flux (Wolff et al., 2006), simulated sea-ice coverage in the Southern Ocean, and computed annual mean Southern Ocean net shortwave forcing over precession band (23 kyr)

Parameters	Coherency (lower/higher)	Phase (º)	Phase (kyr)
$\Delta BWT_{MD05\text{-}2920}$			
Sea salt flux	0.81 (0.40/0.95)	11.1±0.4	0.7±0.0
Simulated sea-ice	0.86 (0.54/0.96)	59.3±50.6	3.8±3.2
Shortwave forcing	0.87 (0.57/0.97)	15.5±7.3	1.0±0.5
$\Delta BWT_{ODP1123}$			
Sea salt flux	0.85 (0.51/0.96)	6.8±2.3	0.4±0.1
Simulated sea-ice	0.91 (0.68/0.98)	55.8±49.2	3.6±3.1
Shortwave forcing	0.92 (0.71/0.98)	13.6±6.8	0.8±0.4

Analyses were carried out using the Blackman-Tukey method with a bandwidth of 0.010 kyr^{-1} and a confidence interval of 95%. No-zero coherence > 0.603.

Supplementary figure caption:

Figure S1. Comparison of the past SST records based on foraminiferal Mg/Ca with zoom for the last four terminations ODP806B (0º19.1'N, 159º21.7'E, 2520 m; (Lea et al., 2000), MD97-2140 (2º02'N, 141º46'E, 2547 m; (de Garidel-Thoron et al., 2005), MD98-2162, (4º41.33'S, 117º54.17'E, 1855m; (Visser et al., 2003), MD01-2378 (13°4.95′S, 121°47.27′E, 1783 m; (Xu et al., 2008) and MD06-3067 (6°31′N, 126°30′E, 1575 m; (Bolliet et al., 2011).

Figure S2. Mg/Ca (mmol/mol) of *G. ruber* for the past 400 kyr together with individual foraminiferal test weight (250-355 μm) and loss of the tests during the cleaning. Bleu zones are glacial periods and numbers along upper x-axis indicate marine isotopic stages.

Figure S3. (a) Correlation between Nino 3.4 SSTA and tropical West Pacific SSTA field obtained from the Reynolds SST data set (Vazquez-Cuervo et al., 1998). (b) Present-day Monthly sea surface salinity in upper 50 m at 2.5S and 144.5E (Antonov et al., 2010). (c) Monthly climatological Chlorophyll-a concentration (1998/01 - 2007/12) at 2.9S and 144.4E. Data from http://oceancolor.gsfc.nasa.gov/.

Figure S4. Comparison between the simulated ice volume by gLOVE over the last 406 ka with reconstructed sea level evolution (Siddall et al., 2003; Waelbroeck et al., 2002).

Figure S5. Spectral analysis (multitaper method, MTM and Blackmann-Tuckey) of *G. ruber* Mg/Ca SST of core MD05-2920 performed with the Analyseries 2.0 software (Paillard et al., 1996). The power spectra and the significance value (>0.95) of the peaks clearly show that dominant frequencies correspond to the obliquity (41 kyr), the precession (23 kyr) and 100 kyr. Non-primary spectral peak represents the heterodyne of obliquity and the 23 kyr component of precession (1/41+1/23 = 1/14.7) also appears with semi-precession band (11 kyr) although these peaks are much smaller. BW=Band Width.

Figure S6. Comparison between residual Mg/Ca-SST variability that is unrelated to CO_2 forcing and seasonal SST bias related to *G. ruber* production over the past 400 kyr. The seasonal bias is estimated from chlorophyll-weighted simulated seasonal SSTs: $\Sigma_{i=1,4}$ chl(i) SST(i,t)/$\Sigma_{i=1,4}$ chl(i), with chl(i) representing the observed SeaWiFS seasonal mean chlorophyll concentration (Figure S2c) during December-January-February (i=1), March-April-May (i=2), June-July-August (i=3), September-October-November (i=4) and SST(i,t) representing the SST in TR400 in season i and year t. The small seasonal bias and anti-relationship with the residual Mg/Ca-SST indicate that the seasonality is not the reason for residual Mg/Ca-SST variability.

Figure S7. Relationship between Antarctic air temperature anomaly relative to the present and WPWP SST anomaly for the last 400 kyr. Proxy relationship between Mg/Ca-SST of core MD05-2920 and the deuterium-based temperature reconstructions from Antarctica (Jouzel et al., 2007) is characterized by a slope of 2.9 (R^2=0.7). The simulated relationship based on TR400 shows a very similar slope of 2.8 (R^2=0.5)

Reference

Paillard, D., Labeyrie, L., and Yiou, P.: Macintosh program performs time-series analysis, EOS Trans. AGU, 77, 1996.

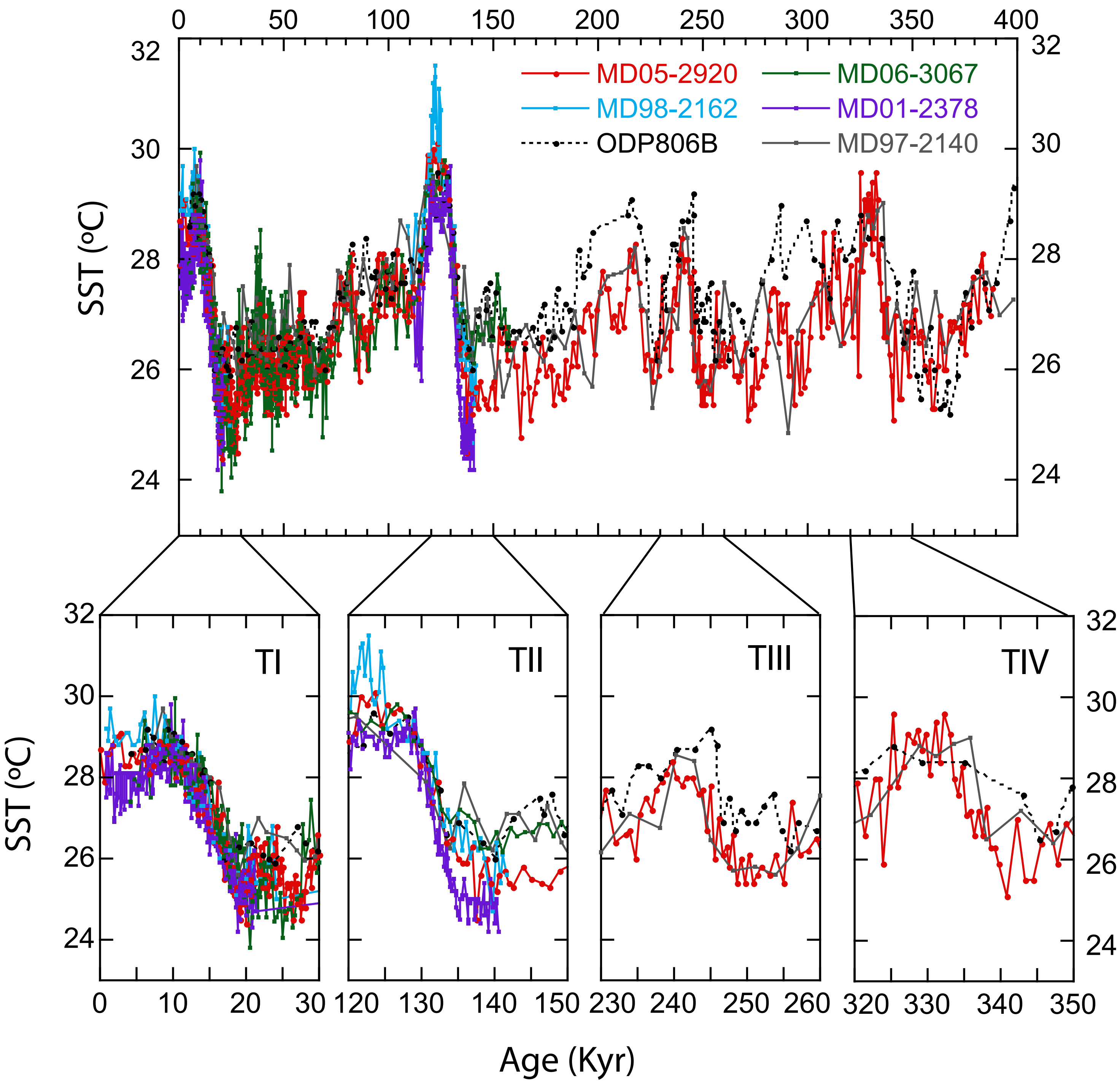
MD05-2920
MD06-3067
MD98-2162
MD01-2378
ODP806B
MD97-2140
SST (ºC)
TI
TII
TIII
TIV
Age (Kyr)

Figure S1

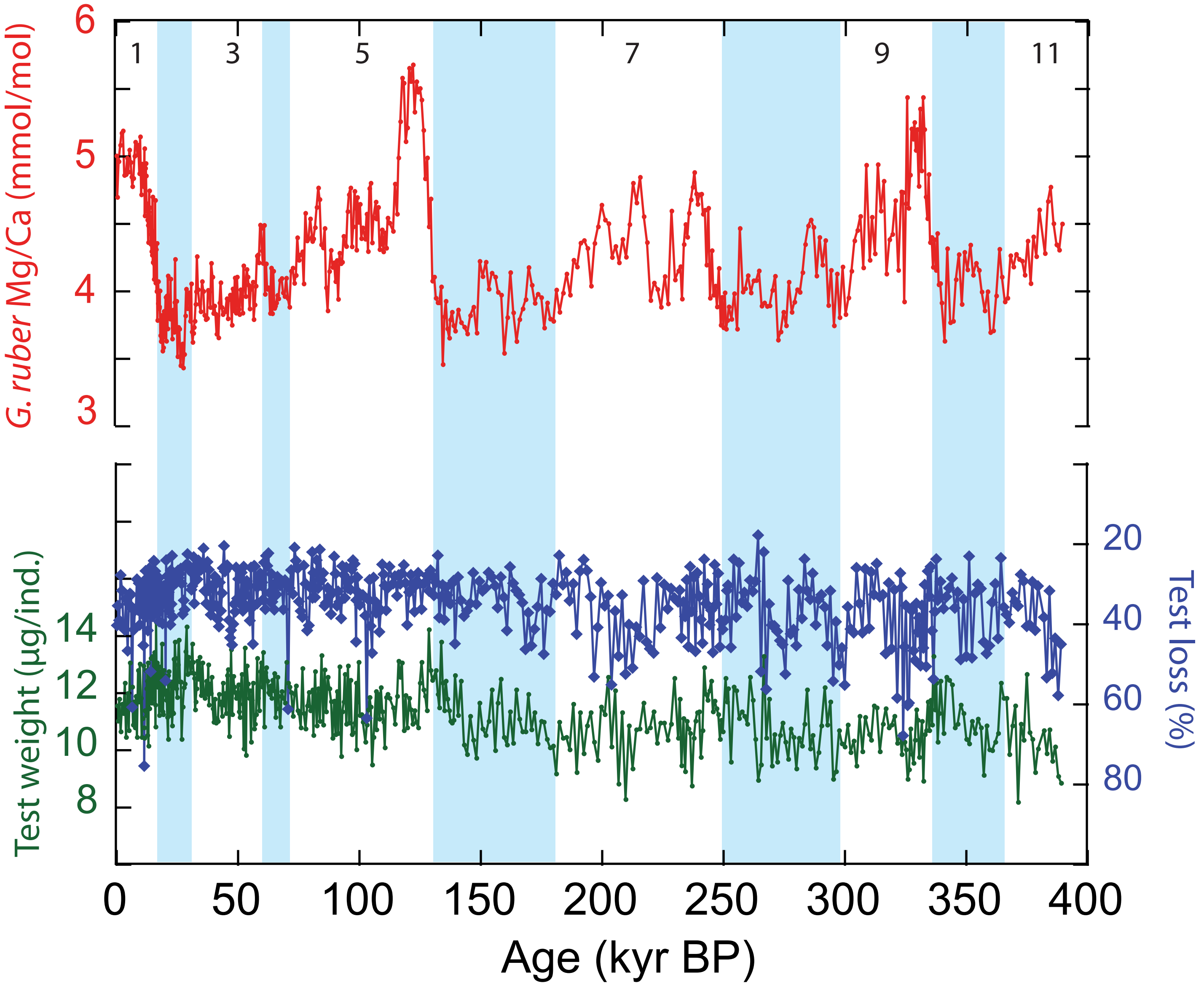

G. ruber Mg/Ca (mmol/mol)
6
5
4
3
1
3
5
7
9
11
Test weight (µg/ind.)
14
12
10
8
Test loss (%)
20
40
60
80
0
50
100
150
200
250
300
350
400
Age (kyr BP)

Figure S2

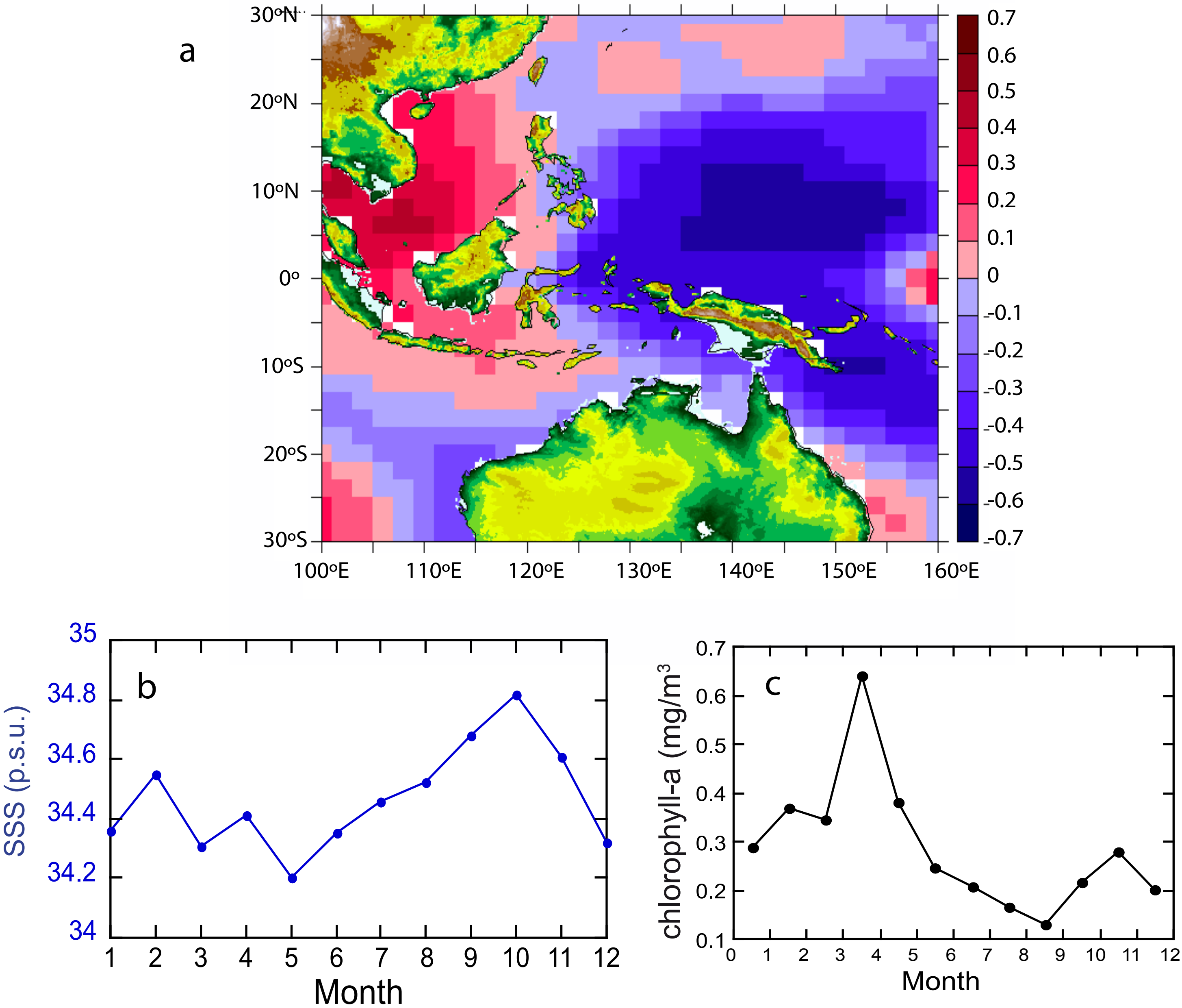
a
30°N
20°N
10°N
0°
10°S
20°S
30°S
100°E
110°E
120°E
130°E
140°E
150°E
160°E
0.7
0.6
0.5
0.4
0.3
0.2
0.1
0
-0.1
-0.2
-0.3
-0.4
-0.5
-0.6
-0.7
b
SSS (p.s.u.)
35
34.8
34.6
34.4
34.2
34
1 2 3 4 5 6 7 8 9 10 11 12
Month
c
chlorophyll-a (mg/m3)
0.7
0.6
0.5
0.4
0.3
0.2
0.1
0 1 2 3 4 5 6 7 8 9 10 11 12
Month

Figure S3

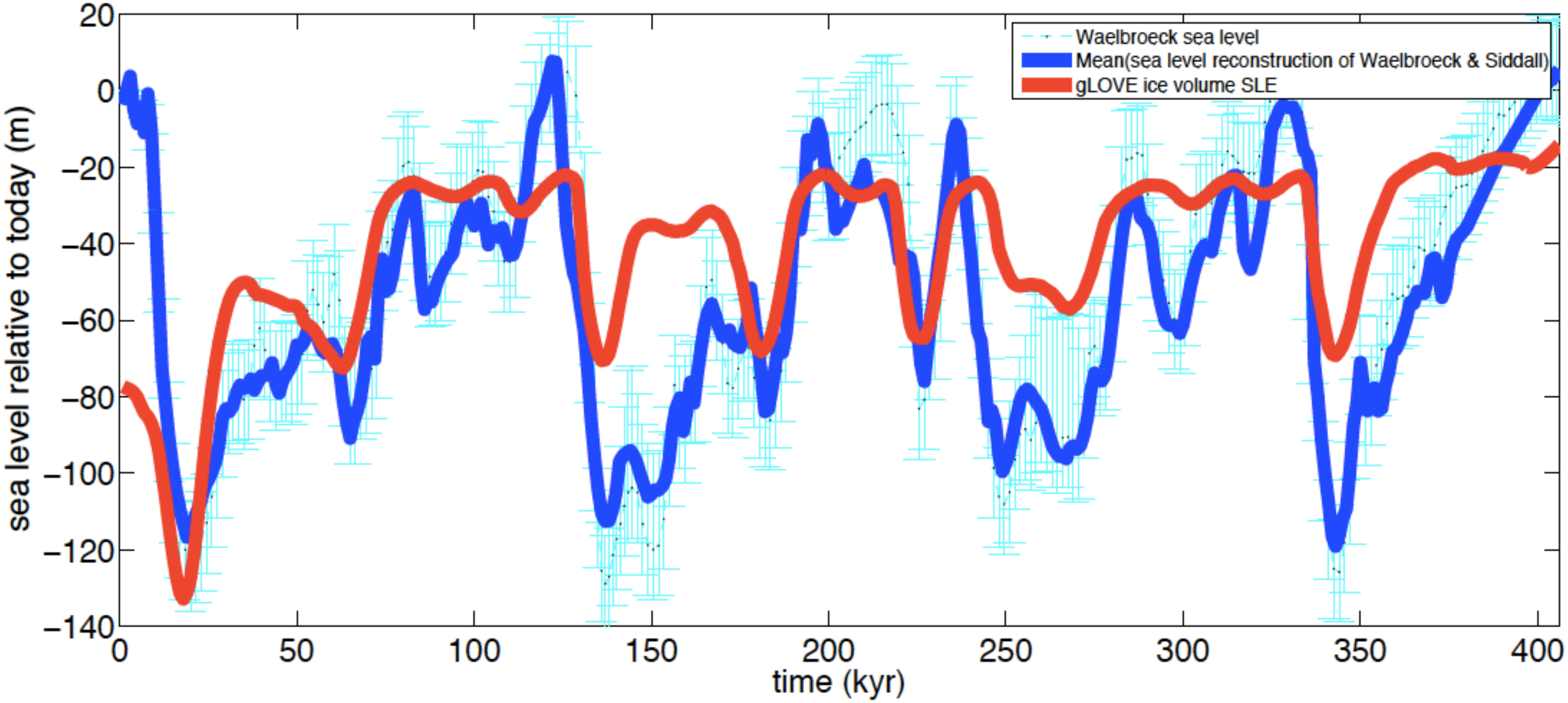

Waelbroeck sea level
Mean(sea level reconstruction of Waelbroeck & Siddall)
gLOVE ice volume SLE
sea level relative to today (m)
time (kyr)
20
0
−20
−40
−60
−80
−100
−120
−140
0
50
100
150
200
250
300
350
400

Figure S4

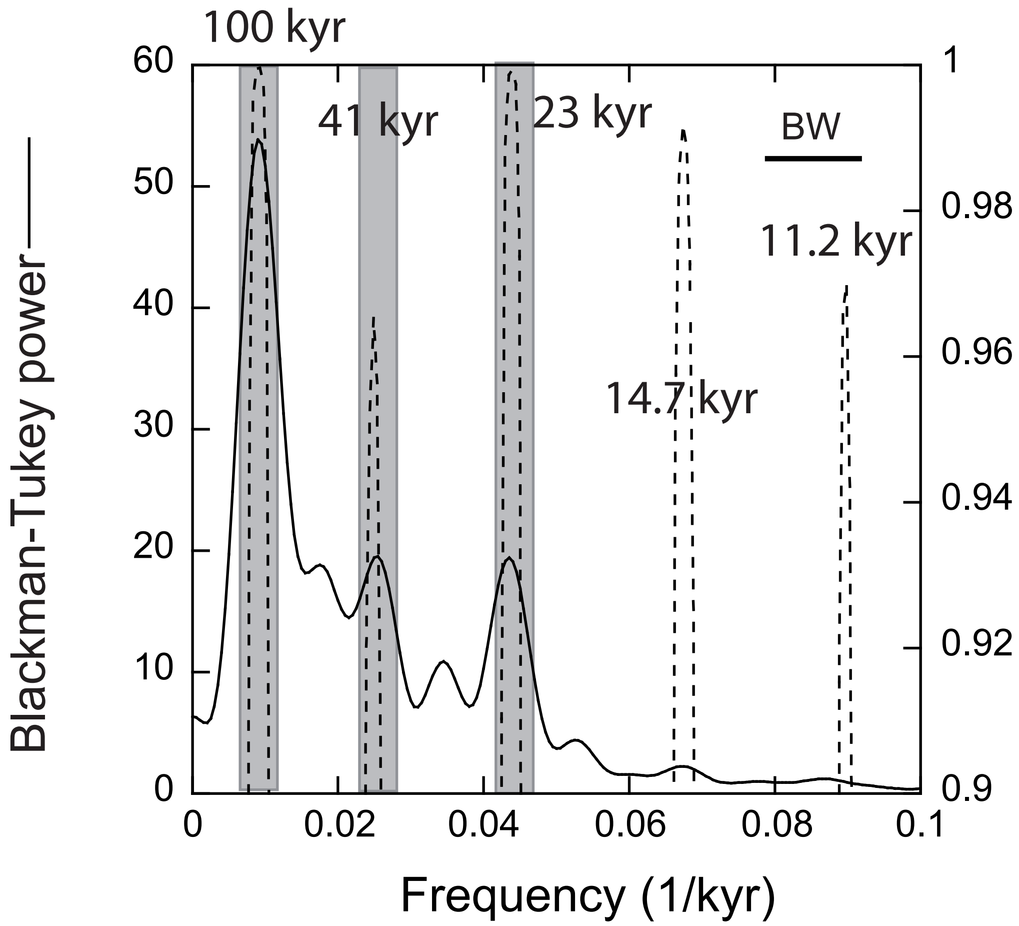

100 kyr
41 kyr
23 kyr
14.7 kyr
11.2 kyr
BW
Blackman-Tukey power
MTM f-test
Frequency (1/kyr)
0
10
20
30
40
50
60
0.9
0.92
0.94
0.96
0.98
1
0
0.02
0.04
0.06
0.08
0.1

Figure S5

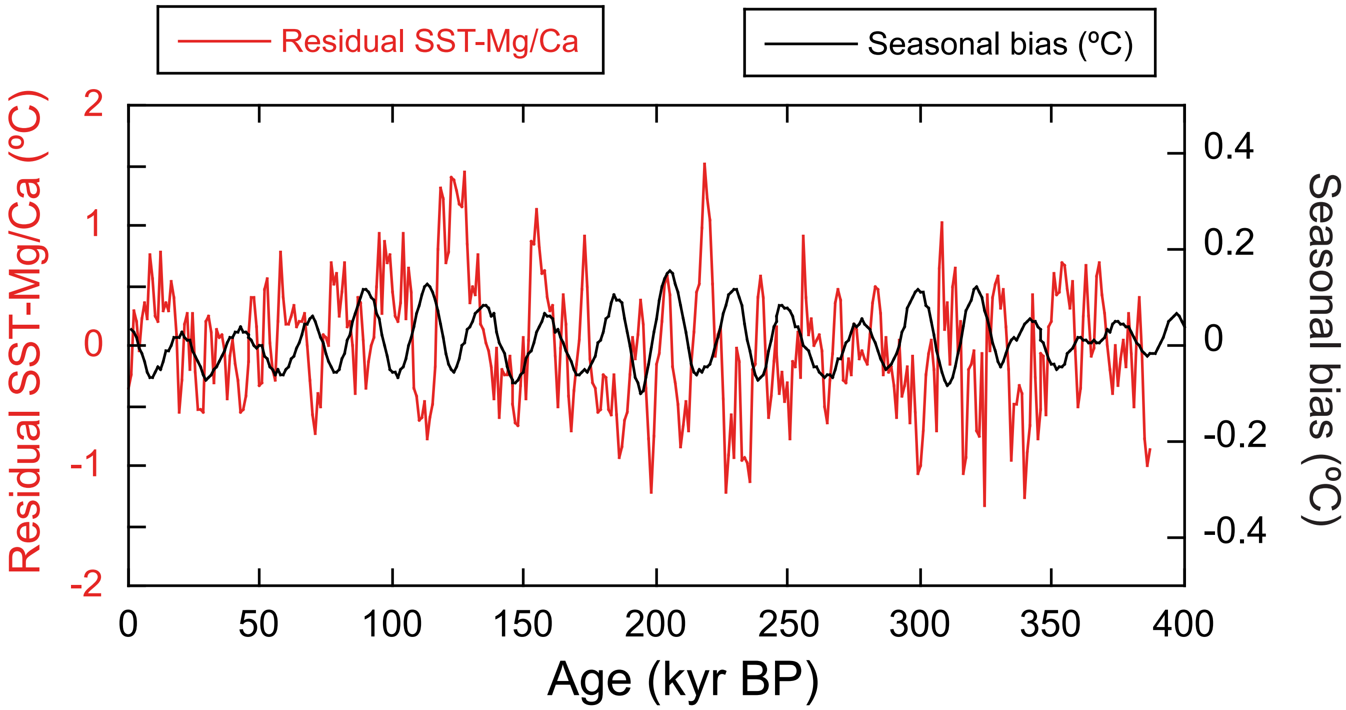

Residual SST-Mg/Ca
Seasonal bias (ºC)
Residual SST-Mg/Ca (ºC)
2
1
0
-1
-2
0.4
0.2
0
-0.2
-0.4
Seasonal bias (ºC)
0
50
100
150
200
250
300
350
400
Age (kyr BP)

Figure S6

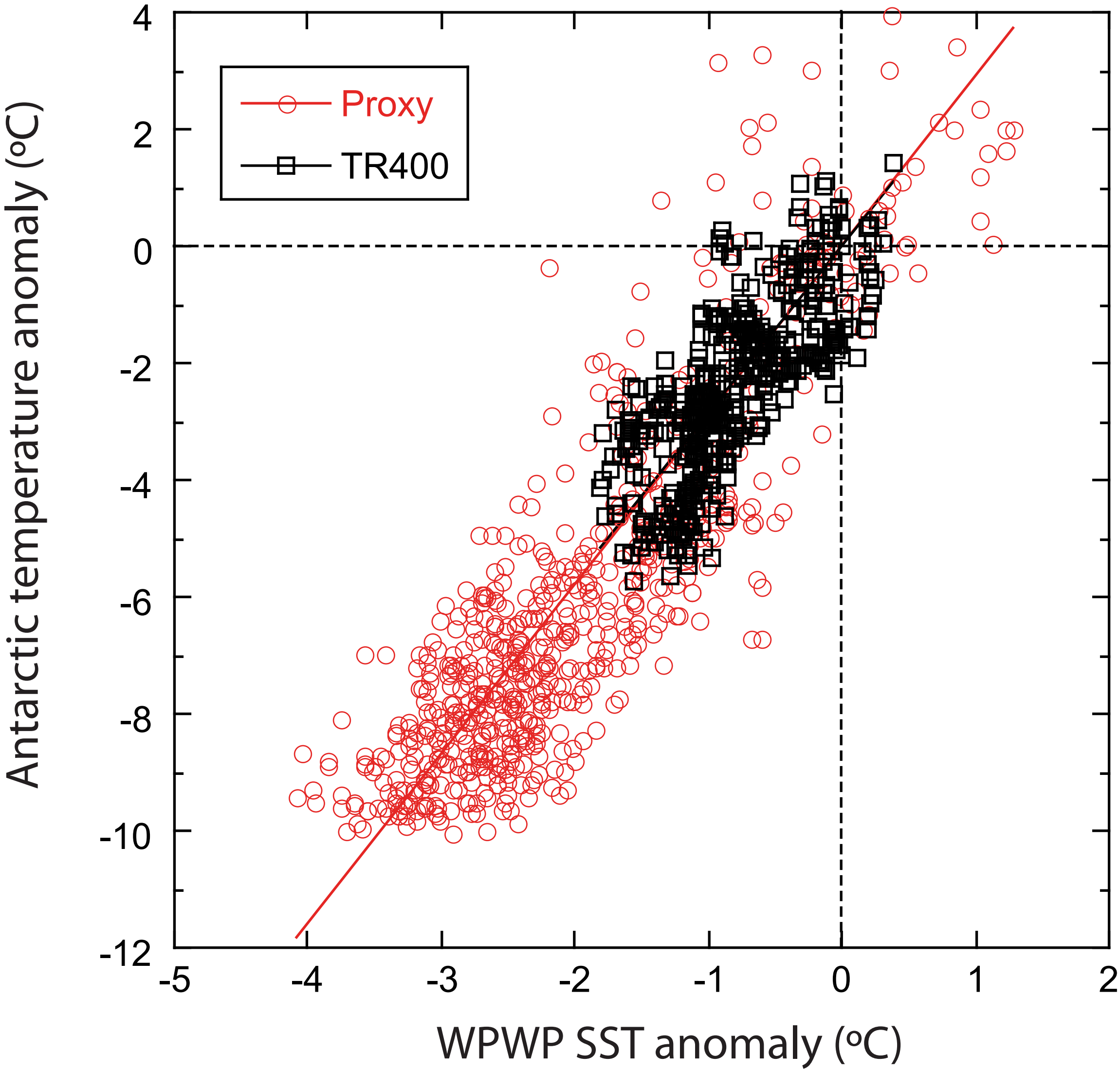
Proxy
TR400
Antarctic temperature anomaly (oC)
WPWP SST anomaly (oC)
4
2
0
-2
-4
-6
-8
-10
-12
-5
-4
-3
-2
-1
0
1
2

Figure S7